

Oxalato-Bridged Dinuclear Complexes of Cr(III) and Fe(III): Synthesis, Structure, and Magnetism of $[(C_2H_5)_4N]_4[MM'(ox)(NCS)_8]$ with $MM' = CrCr, FeFe, \text{ and } CrFe$

Smaïl Triki,^{*,†} Florence Bérézovsky,[†] Jean Sala Pala,^{*,†} Eugenio Coronado,[‡] Carlos J. Gómez-García,[‡] Juan Modesto Clemente,[‡] Amédée Riou,[§] and Philippe Molinié^{||}

UMR CNRS 6521, Chimie, Electrochimie Moléculaires et Chimie Analytique, Université de Bretagne Occidentale, 29285 Brest Cedex, France, Departamento de Química Inorgánica, Universidad de Valencia, Dr. Moliner 50, 46100 Burjasot, Spain, UMR CNRS 6501, Université d'Angers, 49045 Angers Cedex, France, and UMR CNRS 6502, Université de Nantes, 44072 Nantes Cedex, France

Received April 23, 1999

A new series of homo- and heterometallic oxalato-bridged dinuclear compounds of formulas $[Et_4N]_4[MM'(ox)(NCS)_8]$ ($[Et_4N]^+ = [(C_2H_5)_4N]^+$; $ox = C_2O_4^{2-}$) with $MM' = Cr(III)-Cr(III)$ (**1**), $Fe(III)-Fe(III)$ (**2**), and $Cr(III)-Fe(III)$ (**3**) is reported. They have been structurally characterized by infrared spectra and single-crystal X-ray diffraction. The three compounds are isostructural and crystallize in the orthorhombic space group *Cmca* with $Z = 8$, $a = 16.561(8)$ Å, $b = 13.481(7)$ Å, and $c = 28.168(8)$ Å for **1**, $a = 16.515(2)$ Å, $b = 13.531(1)$ Å, and $c = 28.289(4)$ Å for **2**, $a = 16.664(7)$ Å, $b = 13.575(6)$ Å, and $c = 28.386(8)$ Å for **3**. The structure of **3** is made up of a discrete dinuclear anion $[CrFe(ox)(NCS)_8]^{4-}$ and four disordered $[Et_4N]^+$ cations, each of them located on special positions. The anion, in a crystallographically imposed C_{2h} symmetry, contains metal cations in distorted octahedral sites. The $Cr(ox)Fe$ group, which is planar within 0.02 Å, presents an intramolecular metal–metal distance of 5.43 Å. Magnetic susceptibility measurements indicate antiferromagnetic pairwise interactions for **1** and **2** with $J = -3.23$ and -3.84 cm⁻¹, respectively, and ferromagnetic Cr–Fe coupling with $J = 1.10$ cm⁻¹ for **3** (J being the parameter of the exchange Hamiltonian $H = -2JS_1S_2$). The ESR spectra at different temperatures confirm the magnetic susceptibility data.

Introduction

The oxalate group ($C_2O_4^{2-} = ox$) is a very versatile ligand that can adopt a large range of coordination modes.^{1–3} Among those, the bis(bidentate) bridging one is the most interesting for the magnetic interactions; such coordination mode and the ability to transmit electronic effects between magnetic centers as far away as 5 Å constitute the basis for the development of syntheses and magneto–structural investigations of oxalato-bridged compounds.^{4,5} In this context, discrete oxalato-bridged dimers of Cu(II) have been thoroughly studied in magnetochemistry because they provide model systems to test the theories describing the magnetic interactions on a molecular orbital basis.^{6–8} To a lesser extent, other oxalato-bridged dinuclear complexes with divalent metal ions such as nickel, manganese,

iron, and cobalt have been structurally and magnetically characterized.^{9,10} In contrast, examples of dinuclear complexes containing trivalent metal cations of the first row are scarce. Focusing on the homometallic complexes, examples are known with Ti(III),¹¹ Fe(III),^{12–14} and Cr(III).¹⁵ Concerning the heterometallic complexes, to our knowledge, there is no example of Cr(III)–Fe(III) oxalato-bridged dimers, although oxalato heterometallic complexes receive a great deal of attention because of their ability to form two-dimensional and three-dimensional extended networks that behave as ferro- or ferrimagnets.^{16–23} With the aim to clarify the nearest-neighbor exchange interactions occurring in these bimetallic networks,

* To whom correspondence should be addressed. E-mail: sala@univ-brest.fr; triki@univ-brest.fr.

† Université de Bretagne Occidentale.

‡ Universidad de Valencia.

§ Université d'Angers.

|| Université de Nantes.

- (1) Scott, K. L.; Wieghardt, K.; Sykes, A. G. *Inorg. Chem.* **1973**, *12*, 655.
- (2) Le Floch, F.; Sala Pala, J.; Guerschais, J. *Bull. Soc. Chim. Fr.* **1975**, *1–2*, 120.
- (3) Bérézovsky, F.; Hajem, A. A.; Triki, S.; Sala Pala, J.; Molinié, P. *Inorg. Chim. Acta* **1998**, *284*, 8.
- (4) Julve, M.; Verdaguer, M.; Charlot, M. F.; Kahn, O. *Inorg. Chim. Acta* **1984**, *82*, 5.
- (5) Julve, M.; Verdaguer, M.; Gleizes, A.; Philoche-Levisalles, M.; Kahn, O. *Inorg. Chem.* **1984**, *23*, 3808.
- (6) Hay, P. J.; Thibeault, J. C.; Hoffmann, R. *J. Am. Chem. Soc.* **1975**, *97*, 4884.
- (7) Kahn, O. *Angew. Chem., Int. Ed. Engl.* **1985**, *24*, 834.

- (8) Kitagawa, S.; Okubo, T.; Kawata, S.; Kondo, M.; Katada, M.; Kobayashi, H. *Inorg. Chem.* **1995**, *34*, 4790.
- (9) Glerup, J.; Goodson, P. A.; Hodgson, D. J.; Michelsen, K. *Inorg. Chem.* **1995**, *34*, 6255.
- (10) Román, P.; Guzmán-Miralles, C.; Luque, A.; Beitia, J. I.; Cano, J.; Lloret, F.; Julve, M.; Alvarez, S. *Inorg. Chem.* **1996**, *35*, 3741.
- (11) Drew, M. G. B.; Fowles, G. W. A.; Lewis, D. F. *J. Chem. Soc., Chem. Commun.* **1969**, 876.
- (12) Julve, M.; Kahn, O. *Inorg. Chim. Acta* **1983**, *76*, L39.
- (13) Freist, M.; Troyanov, S.; Kemnitz, E. *Inorg. Chem.* **1996**, *35*, 3067.
- (14) Galan-Mascaros, J. R. Ph.D. Thesis, University of Valencia, Burjasot, Spain, 1999.
- (15) Masters, V. M.; Sharrad, C. A.; Bernhardt, P. V.; Gahan, L. R.; Moubaraki, B.; Murray, K. S. *J. Chem. Soc., Dalton Trans.* **1998**, 413.
- (16) Tamaki, H.; Zhong, Z. J.; Matsumoto, N.; Kida, S.; Koikawa, M.; Achiwa, N.; Hashimoto, Y.; Okawa, H. *J. Am. Chem. Soc.* **1992**, *114*, 6974.
- (17) Decurtins, S.; Schmalle, H. W.; Schneuwly, P.; Enslin, J.; Gütlich, P. *J. Am. Chem. Soc.* **1994**, *116*, 9521.
- (18) Decurtins, S.; Schmalle, H. W.; Pellaux, R.; Schneuwly, P.; Hauser, A. *Inorg. Chem.* **1996**, *35*, 1451.

Okawa et al. recently reported a series of oxalato-bridged dinuclear complexes Cr(III)–M(II) (M = Cu, Ni, Co, Fe, Mn).²⁴ In addition to this series, two Cr(III)–Cu(II) dimers²⁵ and one Cr(III)–Ni(II)₃ tetramer,²⁶ as well as an extensive series of M(III)–M(II)–M(III) trimers (M(III) = Fe, Cr; M(II) = Cu, Ni, Co, Fe, Mn)^{27–29} have been reported. For all of them the two metal ions occupy two different coordination sites. In this study of oxalato metal complexes we have prepared the homometallic M(III)–M(III) complexes [Et₄N]₄[Cr₂(ox)(NCS)₈] (**1**) ([Et₄N]⁺ = [(C₂H₅)₄N]⁺) and [Et₄N]₄[Fe₂(ox)(NCS)₈] (**2**) and the first example of the “symmetrical” heterometallic Cr(III)–Fe(III) complex, [Et₄N]₄[CrFe(ox)(NCS)₈] (**3**). Herein are also reported the structure and magnetic properties of these three complexes. The magnetic results, and in particular the ferromagnetic coupling found in **3**, clearly establish that **3** is formed by bimetallic Cr(III)–Fe(III) units and not by a mixture of the two antiferromagnetically coupled homometallic species.

Experimental Section

Materials. Chromium (III) and iron (III) chlorides, iron (II) sulfate, and oxalic acid were purchased from commercial sources and used as received. [Et₄N]₃[Cr(NCS)₆] was prepared according to ref 30.

Syntheses of the Salts 1–3. All reactions were performed under aerobic conditions.

(a) [Et₄N]₄[Cr₂(ox)(NCS)₈] (**1**). A suspension containing stoichiometric amounts of CrCl₃·6H₂O (1.00 g; 3.75 mmol), H₂C₂O₄·2H₂O (0.24 g; 1.88 mmol), KNCS (1.46 g; 15 mmol), and Et₄NCl·2H₂O (1.52 g; 7.5 mmol) in acetone (500 mL) was refluxed under continuous stirring for several hours (ca. 4–5 h). The resulting green solution was immediately filtered, and the green precipitate was washed with cold water and with a small amount of cold acetone. Recrystallization in MeCN gave cubic green crystals (yield ca. 70%). Anal. Calcd for C₄₂H₈₀O₄N₁₂S₈Cr₂: C, 42.83; H, 6.85; N, 14.27; S, 21.78; Cr, 8.83. Found: C, 43.22; H, 7.05; N, 14.24; S, 20.40; Cr, 8.47. IR data [ν/cm⁻¹] on KBr pellets: 2100s(sh) and 2060vs ν(CN), 1645vs ν_{as}(CO), 1350w, and 1300w ν_s(CO), 815m δ(OCO), 480m δ(NCS), 450m δ(OCO), 380s(sh) and 365vs ν(Cr–NCS), 1170m, 1000m, and 780m (Et₄N)⁺. This salt can be also prepared by two other different ways: (i) using a procedure similar to that described above but starting from [Et₄N]₃[Cr(NCS)₆] (1.00 g; 1.26 mmol) and H₂C₂O₄·2H₂O (0.08 g; 0.63 mmol) in acetone (ca. 200 mL); (ii) by reaction in water using a procedure similar to that described to obtain salt **2** but with slight modifications. A solution of CrCl₃·6H₂O (2.00 g; 7.5 mmol) and H₂C₂O₄·2H₂O (0.47 g; 3.75 mmol) in water (40 mL) was boiled with continuous stirring (10 min); then a solution of KNCS (2.92 g; 30 mmol) in water (20

mL) was added. The resulting solution was maintained at boiling temperature (30 min), and Et₄NCl·H₂O (2.76 g; 15 mmol) was added. The brown solid was filtered, washed with water, and dried under vacuum. Recrystallization from dimethylformamide (DMF) gave primarily green rectangular plates of the title compound **1** and after pink rhomboedral crystals of [Et₄N]₃[Cr(NCS)₆]·0.5DMF.

(b) [Et₄N]₄[Fe₂(ox)(NCS)₈] (**2**). FeCl₃ (0.61 g; 3.75 mmol), H₂C₂O₄·2H₂O (0.24 g; 1.88 mmol), and KNCS (1.46 g; 15 mmol) were respectively dissolved in 18, 6.5, and 10 mL of water. The three solutions were mixed with stirring and boiled for 30 min, then solid Et₄NCl·H₂O (1.38 g; 7.5 mmol) was added. The dark-red microcrystalline product was collected by filtration and washed with cold water. Recrystallization by slow evaporation in MeCN gave **2** as black shiny plates that were filtered off and dried under vacuum (yield ca. 60%). Anal. Calcd for C₄₂H₈₀O₄N₁₂S₈Fe₂: C, 42.55; H, 6.80; N, 14.18; S, 21.64; Fe, 9.45. Found: C, 42.33; H, 7.01; N, 14.20; S, 21.30; Fe, 8.95. IR data [ν/cm⁻¹] on KBr pellets: 2080s, 2040vs, and 2020vs ν(CN); 1640vs ν_{as}(CO); 1345w and 1305w ν_s(CO); 800m δ(OCO); 480m δ(NCS); 420w δ(OCO); 295vs, 285vs, and 280vs ν(Fe–NCS); 1170m, 1000m, and 780m (Et₄N)⁺.

(c) [Et₄N]₄[CrFe(ox)(NCS)₈] (**3**). A solution of H₂C₂O₄·2H₂O (0.47 g; 3.75 mmol) in water (10 mL) and a solution of KNCS (2.92 g; 30 mmol) in water (15 mL) were added to a third solution containing CrCl₃·6H₂O (1.00 g; 3.75 mmol) and FeSO₄·7H₂O (1.04 g; 3.75 mmol) in water (30 mL). Powdered Et₄NCl·2H₂O (3.03 g; 15 mmol) and glacial acetic acid (13 mL) were added with vigorous stirring. The resulting mixture was boiled for ca. 1 h. The dark-red precipitate formed was collected by filtration, washed with cold water, and dried under vacuum (yield, ca. 70%). Recrystallization in MeCN gave **3** as black plates with shiny golden iridescence. Anal. Calcd for C₄₂H₈₀O₄N₁₂S₈CrFe (**3**): C, 42.69; H, 6.83; N, 14.23; S, 21.71; Cr, 4.40; Fe, 4.73. Found: C, 42.39; H, 6.80; N, 14.07; S, 21.86; Cr, 4.40; Fe, 5.00. Supplementary microanalyses have been performed on four samples corresponding to four different syntheses. The results, given as Cr %, Fe %, and Cr/Fe ratio, are the following: sample **A**, 4.69, 4.40, 1.14; sample **B**, 4.63, 4.40, 1.12; sample **C**, 4.12, 4.62; 0.96; sample **D**, 4.57, 4.90, 1.00. IR data [ν/cm⁻¹] on KBr pellets: 2100s, 2070vs, and 2020vs ν(CN); 1650vs ν_{as}(CO); 1350w and 1310w ν_s(CO); 805m δ(OCO); 480m δ(NCS); 430w δ(OCO); 380s(sh) and 365vs ν(Cr–NCS); 295vs, 285vs, and 280vs ν(Fe–NCS); 1170m, 1000m, and 780m (Et₄N)⁺.

Physical Techniques. Infrared spectra were recorded in the range 4000–200 cm⁻¹ using a Perkin-Elmer 1430 spectrophotometer with samples prepared as KBr pellets. The magnetic studies were carried out on powder samples enclosed in medical caps. The magnetic susceptibility measurements were performed at 0.1 T after zero-field cooling, in the temperature range 2–300 K with a superconducting quantum interference device (SQUID) magnetometer MPMS-XL-5 from Quantum Design Corporation. The molar susceptibility was corrected for the sample holder and diamagnetic contributions of all atoms. Variable temperature ESR spectra were recorded at X-band in polycrystalline samples with a Bruker ER200 spectrometer equipped with a helium cryostat. Elemental analyses were obtained from the Service Central d'Analyses, CNRS, Vernaison, France.

X-ray Crystallography. Preliminary studies showed that the three compounds **1**, **2**, and **3** were isostructural with $a = 16.561(8)$ Å, $b = 13.481(7)$ Å, and $c = 28.168(8)$ Å for **1**, $a = 16.515(2)$ Å, $b = 13.531(1)$ Å, and $c = 28.289(4)$ Å for **2**, $a = 16.664(7)$ Å, $b = 13.575(6)$ Å, and $c = 28.386(8)$ Å for **3**. A black prismatic crystal of **3** with dimensions 0.15 × 0.11 × 0.10 mm³ was mounted on an Enraf-Nonius CAD4 automatic diffractometer with graphite-monochromator Mo Kα radiation ($\lambda = 0.71073$ Å). Cell dimensions were obtained from 25 reflections with a 2θ angle in the range 9.70–23.88°. A total of 3130 reflections were collected ($h, 0-19; k, 0-16; l, 0-33$) in the 2θ range 4.12–49.96° using $\theta/2\theta$ scan mode. During the data collection, three standard reflections were measured every 120 min and showed no significant decay. No absorption correction was applied. On the basis of systematic absences and statistics of intensity distribution, the space group was found to be *Cmca*. The structure was solved by SIR92; subsequent difference Fourier syntheses led to the location of all non-hydrogen atoms.³¹ All non-hydrogen atoms were refined on F^2 by weighted anisotropic full-matrix least-squares methods with SHELXL-

- (19) Decurtins, S.; Pellaux, R.; Hauser, A.; von Arx, M. E. In *Magnetism: A Supramolecular Function*; Kahn, O., Ed.; NATO ASI Series C484; Kluwer Academic Publishers: Dordrecht, The Netherlands, 1996; p 487.
- (20) Mathonière, C.; Nuttall, C. J.; Carling, S. G.; Day, P. *Inorg. Chem.* **1996**, *35*, 1201.
- (21) Carling, S. G.; Mathonière, C.; Day, P.; Abdul Malik, K. M.; Coles, S. J.; Hursthouse, M. B. *J. Chem. Soc., Dalton Trans.* **1996**, 1839.
- (22) Pellaux, R.; Schmalle, H. W.; Huber, R.; Fischer, P.; Hauss, T.; Ouladdiaf, B.; Decurtins, S. *Inorg. Chem.* **1997**, *36*, 2301.
- (23) Clemente-León, M.; Coronado, E.; Galán-Mascarós, J. R.; Gómez-García, C. J. *J. Chem. Soc., Chem. Commun.* **1997**, 1727.
- (24) Ohba, M.; Tamaki, H.; Matsumoto, N.; Okawa, H. *Inorg. Chem.* **1993**, *32*, 5385.
- (25) Ohba, M.; Tamaki, H.; Matsumoto, N.; Okawa, H.; Kida, S. *Chem. Lett.* **1991**, 1157.
- (26) Pei, Y.; Journaux, Y.; Kahn, O. *Inorg. Chem.* **1989**, *28*, 1000.
- (27) Coronado, E.; Galán-Mascarós, J. R.; Giménez-Saiz, C.; Gómez-García, C. J.; Ruiz-Pérez, C.; Triki, S. *Adv. Mater.* **1996**, *8*, 737.
- (28) Coronado, E.; Galán-Mascarós, J. R.; Giménez-Saiz, C.; Gómez-García, C. J. In *Magnetism: A Supramolecular Function*; Kahn, O., Ed.; NATO ASI Series C484; Kluwer Academic Publishers: Dordrecht, The Netherlands, 1996; p 281.
- (29) Coronado, E.; Galán-Mascarós, J. R.; Giménez-Saiz, C.; Gómez-García, C. J. *Synth. Met.* **1997**, *85*, 1677.
- (30) Sabatini, A.; Bertini, I. *Inorg. Chem.* **1965**, *4*, 959.

Table 1. Crystallographic Data for $[\text{Et}_4\text{N}]_4[\text{CrFe}(\text{C}_2\text{O}_4)(\text{NCS})_8]$ (**3**)

chemical formula ^a	$\text{CrFeC}_{42}\text{H}_{80}\text{N}_{12}\text{S}_8\text{O}_4$	fw ^a	1181.52
<i>a</i> , Å	16.664(7)	space group	<i>Cmca</i> (No. 64)
<i>b</i> , Å	13.575(6)	temp, K	296
<i>c</i> , Å	28.386(8)	λ , Å	0.710 73
<i>V</i> , Å ³	6421(4)	ρ_{calc} , g cm ⁻³	1.222
<i>Z</i> ^a	4	μ , cm ⁻¹	6.99
<i>R</i> (<i>F</i> _o) ^b	0.088	<i>R</i> _w (<i>F</i> _o ²) ^c	0.215

^a There is 0.5 chemical formula in the asymmetric unit. ^b $R = \sum |F_o - F_c|/F_o$. ^c $R_w = [(\sum wF_o^2 - F_c^2)^2 / w(F_o^2)^2]^{1/2}$.

Table 2. Selected Bond Distances (Å) and Angles (deg) in **3**^a

M—N1	2.004(15)	S3—C3	1.636(14)
M—N2	2.041(16)	N1—C1	1.146(15)
M—N3	1.932(11)	N2—C2	1.132(18)
M—O4	2.056(6)	N3—C3	1.132(12)
S1—C1	1.613(17)	O4—C4	1.264(7)
S2—C2	1.59(2)	C4—C4(i)	1.53(3)
N1—M—N2	173.0(5)	N3—M—N3(*)	97.5(6)
N1—M—N3	91.7(4)	N3—M—O4	91.2(3)
N1—M—O4	88.7(3)	N3—M—O4(*)	171.3(3)
N2—M—N3	92.9(4)	N2—M—O4	86.0(3)
O4—M—O4(*)	80.1(3)	N1—C1—S1	178.6(16)
N2—C2—S2	177.6(19)	N3—C3—S3	177.6(11)

^a Code of equivalent positions: (i) = 1 - *x*, -*y*, -*z*; (*) = 1 - *x*, *y*, *z*. *M* = 1/2(Cr + Fe).

97 using 794 independent reflections with $I \geq 2\sigma(I)$.³² In the final difference map, the deepest hole was $-0.269 \text{ e } \text{Å}^{-3}$ and the highest peak $0.327 \text{ e } \text{Å}^{-3}$. The Cr(III) and the Fe(III) cations were considered as equally located on two equivalent metallic positions. The disordered tetraethylammonium cations were located on special positions (0 *y z* and 1/4 1/4 0), and therefore, the hydrogen atoms were not included in the refinement. Scattering factors and corrections for anomalous dispersion were taken from the *International Tables for X-ray Crystallography*.³³ The drawings were made with ORTEP.³⁴ All calculations were performed on Alphastation 255 4/233 computer. Brief crystal data and selected bond distances and bond angles are listed in Tables 1 and 2, respectively. Complete crystallographic details are included in the Supporting Information.

Results and Discussion

Syntheses and General Characterization. (a) Homometallic Compounds (1 and 2). The chromium (III) compound **1** ($[\text{Et}_4\text{N}]_4[\text{Cr}_2(\text{ox})(\text{NCS})_8]$) was prepared by a one-pot reaction between chromium chloride, $\text{CrCl}_3 \cdot 6\text{H}_2\text{O}$, potassium thiocyanate, KNCS, oxalic acid, $\text{H}_2\text{C}_2\text{O}_4 \cdot 2\text{H}_2\text{O}$, and tetraethylammonium chloride, $\text{Et}_4\text{NCl} \cdot 2\text{H}_2\text{O}$, in acetone. Recrystallization of the resulting precipitate in acetonitrile afforded **1** as green crystals in ca. 70% yield. Similar reaction performed in water gave a mixture of **1** and pink crystals of $[\text{Et}_4\text{N}]_3[\text{Cr}(\text{NCS})_6] \cdot 0.5\text{DMF}$ after recrystallization in dimethylformamide. The iron (III) analogue **2**, $[\text{Et}_4\text{N}]_4[\text{Fe}_2(\text{ox})(\text{NCS})_8]$, was similarly prepared in water using ferric chloride FeCl_3 . After recrystallization in acetonitrile, **2** appeared as black plates with brilliant golden iridescence.

Heterometallic Compound 3. Reactions starting from a $\text{CrCl}_3 \cdot 6\text{H}_2\text{O}$ and $\text{FeSO}_4 \cdot 7\text{H}_2\text{O}$ 1/1 mixture in water afforded in a reproducible way samples having, within the experimental error, a Cr/Fe ratio of 1 (cf. Experimental Section). Therefore,

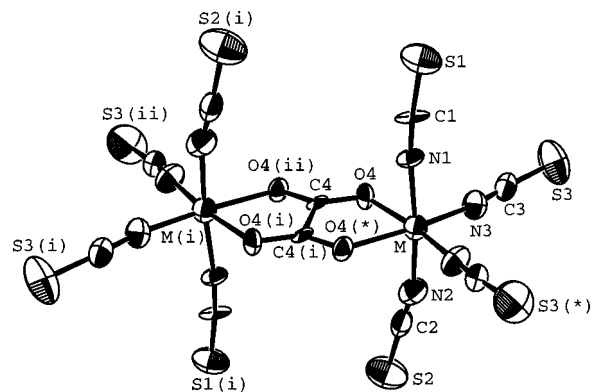


Figure 1. ORTEP drawing of the dinuclear anion $[\text{CrFe}(\text{ox})(\text{NCS})_8]^{4-}$ of **3** with the atom-numbering scheme [$M = 1/2(\text{Cr} + \text{Fe})$]. Atoms are represented by their displacement ellipsoids with 50% probability level. Code of equivalent positions: (i) = 1 - *x*, -*y*, -*z*; (ii) = *x*, -*y*, -*z*; (*) = 1 - *x*, *y*, *z*.

formation of the bimetallic compound $[\text{Et}_4\text{N}]_4[\text{CrFe}(\text{ox})(\text{NCS})_8]$ (**3**) as a result of the aerobic oxidation of iron (II) was taken into consideration. It is worthy to note that in this synthesis an iron (II) salt had to be used. Reactions starting from a 1/1 mixture of $\text{CrCl}_3 \cdot 6\text{H}_2\text{O}$ and FeCl_3 afforded samples having a variable composition and Cr/Fe ratios between 0.25 and 1.6. Therefore, synthesis of compound **3** seems to require a very high excess of Cr(III) throughout the reaction. This condition was fulfilled here by slow aerobic oxidation of the ferrous cations.

IR Spectra. The IR spectra of compounds **1–3** obviously present the characteristic absorptions of the oxalato-bridged group, the isothiocyanato ligand, and the tetraethylammonium cation. For the oxalate ligand, the spectra of **1–3** exhibit a strong $\nu_{\text{as}}(\text{OCO})$ band near 1650 cm^{-1} , a weak $\nu_{\text{s}}(\text{OCO})$ doublet in the $1300\text{--}1350 \text{ cm}^{-1}$ range, and a medium $\delta(\text{OCO})$ band near 810 cm^{-1} . The positions of these absorptions and the important splitting in the doublet (ca. 40 cm^{-1}) are very similar to those observed in other bis(bidentate) oxalato complexes.^{3,35} They indicate for the oxalate ligand a symmetry higher than that of the classical bidentate ligand. For the thiocyanate groups, the $\delta(\text{NCS})$ value of 480 cm^{-1} found in compounds **1–3** clearly indicates that NCS groups are bonded to the metal ion through the nitrogen atoms because N-bonded groups absorb in the range $440\text{--}490 \text{ cm}^{-1}$; S-bonded groups absorb in the range $400\text{--}440 \text{ cm}^{-1}$.^{30,36–38}

Crystal Structures. Since preliminary studies indicated that compounds **1–3** were isostructural (Experimental Section), single crystal structure determination was only performed on the heterometallic derivative **3**. The structure of **3** consists of disordered $(\text{Et}_4\text{N})^+$ cations located on special positions and binuclear $[\text{M}_2(\text{ox})(\text{NCS})_8]^{4-}$ anions located on a crystallographic $2/m$ special position.

Assuming that the two metallic positions are crystallographically equivalent ($M = 1/2\text{Cr} + 1/2\text{Fe}$), the anion, which includes a bis(bidentate) oxalate ligand, has a crystallographically imposed C_{2h} symmetry with the 2-fold axis perpendicular to the plane containing the four NCS axial ligands (Figure 1). Each metal cation presents a distorted octahedral environment com-

(31) *OpenMoleN, Interactive Structure Solution*; Nonius B. V.: Delft, The Netherlands 1997.

(32) Sheldrick, G. M. *SHELXL-97, Program for Crystal Structure Refinement*; Universität Göttingen: Göttingen, Germany, 1997.

(33) *International Tables for X-Ray Crystallography*; Kynoch Press: Birmingham, U.K. 1975; Vol. 4.

(34) Johnson, C. K. *ORTEP*; Report ONL-3794; Delft, The Netherlands, 1985.

(35) Tamaki, H.; Zhong, Z. J.; Matsumoto, N.; Kida, S.; Koikawa, M.; Achiwa, N.; Hashimoto, Y.; Okawa, H. *J. Am. Chem. Soc.* **1992**, *114*, 6974.

(36) Clark, R. J. H.; Williams, C. S. *Spectrochim. Acta* **1966**, *22*, 1081.

(37) Buckley, R. C.; Wardeska, J. G. *Inorg. Chem.* **1972**, *11*, 1723.

(38) Bailey, R. A.; Kozak, S. L.; Michelsen, T. W.; Mills, W. N. *Coord. Chem. Rev.* **1971**, *6*, 407.

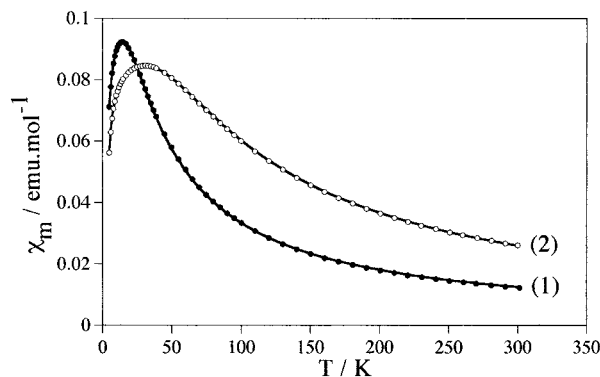


Figure 2. Thermal variation of the molar susceptibilities for complexes **1** and **2** in the form χ_m vs T : (open and full circles) experimental results; (solid lines) best theoretical fit.

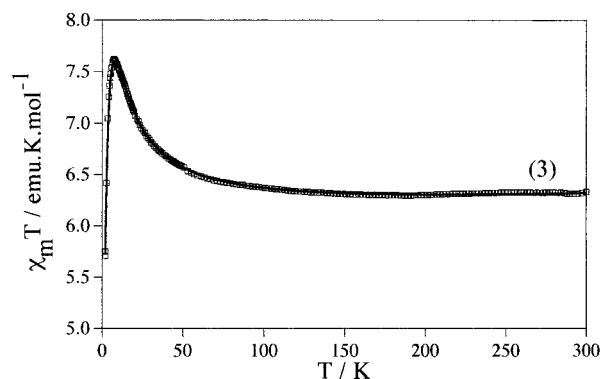


Figure 3. Thermal variation of the molar susceptibility for complex **3** in the form $\chi_m T$ vs T : (squares) experimental results; (solid line) best theoretical fit.

prising two oxygen atoms of the oxalate group and four nitrogen atoms of isothiocyanate ligands. The central unit $M(\text{ox})M$ is planar within 0.02 Å; the distances of the N3, C3, and S3 atoms to this least-squares plane are respectively -0.05 , $+0.07$, and $+0.23$ Å (or $+0.05$, -0.07 , and -0.23 Å). The $M\text{---}O4$ bond length of 2.056 Å and the $M\cdots M$ intramolecular distance of 5.41 Å are between those reported for the bis(bidentate) oxalato $\text{Cr(III)}\text{---}\text{Cr(III)}$ and $\text{Fe(III)}\text{---}\text{Fe(III)}$ homometallic complexes $[\text{Cr}_2(\text{ox})_5]^{4-}$ (2.035 and 5.32 Å, respectively)¹⁵ and $[\text{Fe}_2(\text{ox})_5]^{4-}$ (2.082 and 5.47 Å, respectively).¹⁴ For the isothiocyanate ligands, the $M\text{---}N$ axial bond lengths (2.00 and 2.04 Å) are slightly longer than the equatorial ones in the trans positions of the oxalate group (1.93 Å) (Table 2).

(b) Magnetic Properties. The magnetic properties of these salts are depicted in Figures 2 and 3 with plots of χ_m vs T and $\chi_m T$ vs T . For **1** and **2** the molar susceptibility shows a rounded maximum at 15 and 30 K, respectively (Figure 2), while $\chi_m T$ reveals a continuous decrease respectively for **1** and **2** from values of 3.7 and 7.8 emu K mol^{-1} at 300 K to values close to zero at 2 K. This is characteristic of an antiferromagnetic exchange interaction between two metal centers. In contrast, for **3** the $\chi_m T$ product shows an increase from a value of 6.3 emu K mol^{-1} at 300 K to a value of 7.6 emu K mol^{-1} at 7 K, where it exhibits a sharp maximum followed by a strong decrease at lower temperatures (Figure 3). The room-temperature value is close to that expected for a pair of uncoupled $\text{Cr(III)}\text{---}\text{Fe(III)}$ centers (with $S_{\text{Cr}} = 3/2$ and $S_{\text{Fe}} = 5/2$), while the increase in $\chi_m T$ indicates that the $\text{Cr(III)}\text{---}\text{Fe(III)}$ exchange interaction is ferromagnetic.

To treat these data, we have used the susceptibility expressions derived for spin pairs ($3/2\text{---}3/2$, $5/2\text{---}5/2$, and $3/2\text{---}5/2$ for **1**–**3**, respectively) coupled through an isotropic exchange interaction

Table 3. Best-Fit Values in **1**–**3**

compounds	J, cm^{-1}	g	θ, cm^{-1}	$\rho, \%$	$N\alpha, \text{emu mol}^{-1}$
1 ^a	-3.23	1.989			610×10^{-6}
2 ^b	-3.84	2.00		0.5	
3 ^c	$+1.10$	1.97	-0.97		547×10^{-6}

^a $\chi_m = \chi_D + N\alpha$. ^b $\chi_m = (1 - \rho)\chi_D + \rho(35N\beta^2g^2/(12kT))$. ^c $\chi_m = \chi_D T/(T - \theta) + N\alpha$, where the dimer susceptibility χ_D can be easily obtained for any isotropic dimer. See ref 39.

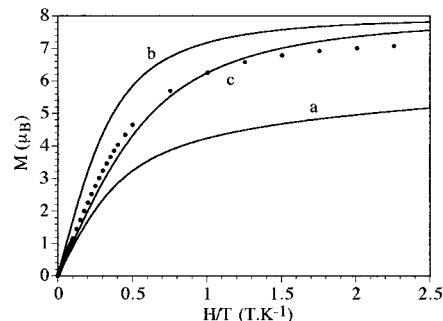


Figure 4. Isothermal magnetization of compound **3** at 2 K. Solid lines are the behavior of a ferromagnetic dimer with $J = 0.83 \text{ cm}^{-1}$ and $D = 6.3 \text{ cm}^{-1}$ (a), a Brillouin function for an $S = 4$ spin state corrected to account for a molecular field parameter $\theta = -1.39 \text{ K}$ with $g = 1.97$ (the values found in the fitting of the $\chi_m T$ curve) (b), and the fit to a Brillouin function with a reduced effective g value of 1.785 (see text) (c).

J (the Hamiltonian is written as $H = -2JS_1S_2$).³⁹ The best fits are plotted as solid lines in Figures 2 and 3, and the resulting parameters are summarized in Table 3. For **1** an excellent description of the data in the whole temperature range (2–300 K) has been obtained when the exchange parameter is $J = -3.23 \text{ cm}^{-1}$. In the fitting procedure the g parameter has been fixed to the value obtained from ESR ($g = 1.989$). The J value is close to that found in the related complex anion $[\text{Cr}_2(\text{ox})_5]^{4-}$ ($J = -3.1 \text{ cm}^{-1}$) recently reported.¹⁵ A temperature-independent paramagnetic (TIP) term $N\alpha = 610 \times 10^{-6} \text{ emu mol}^{-1}$ also had to be considered in the fit to better reproduce the high-temperature behavior. For **2** a similar procedure has enabled us to obtain an antiferromagnetic exchange parameter $J = -3.84 \text{ cm}^{-1}$ and a g value of 2.00. This J value is also in the range of those observed in the other two examples of $\text{Fe(III)}\text{---}\text{Fe(III)}$ oxalato-bridged complexes that are known (-3.61 cm^{-1} in $[\text{Fe}_2(\text{acac})_4(\text{ox})]\cdot 0.5\text{H}_2\text{O}$ and -3.56 cm^{-1} in $[\text{Fe}_2(\text{ox})_5]^{4-}$).^{12,14} A small amount of paramagnetic monomeric impurity (0.5%) had to be introduced to fit the data. This impurity was also detected by ESR (see below). Finally, for **3** a model that assumes a ferromagnetic exchange interaction $J = 1.10 \text{ cm}^{-1}$ and a g value of 1.97 provides a good description of the magnetic data down to 7 K. Below this temperature, the model predicts a plateau because the ground state of the cluster is $S = 4$. However, the experimental data exhibit a sharp decrease. Such a feature is well reproduced by introducing in the model a molecular field parameter θ that accounts for the presence of weak antiferromagnetic intercluster interactions. A θ value of -1.39 K (-0.97 cm^{-1}) is then obtained. Emphasis is placed in the need of this parameter to explain the low-temperature behavior rather than in the resulting value. In fact, single ion anisotropy should also contribute to this decrease in $\chi_m T$. To examine to which extent single ion anisotropy effects account for the observed behavior, we have fitted the data to a model that considers both an

(39) Kahn, O. *Molecular Magnetism*; VCH: New York, 1993.

(40) Borrás-Almenar, J. J.; Clemente-Juan, J. M.; Coronado, E.; Tsukerblat, B. S. *Inorg. Chem.* **1999**, *38*, 6081.

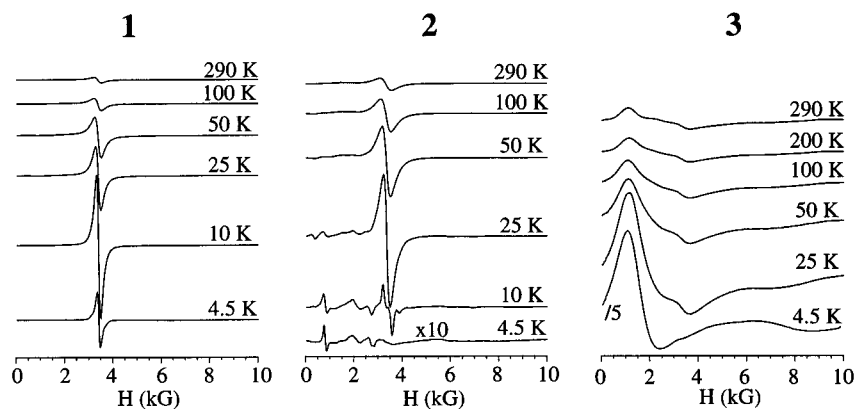


Figure 5. EPR spectra of compounds 1–3 at different temperatures.

exchange parameter and a zero-field splitting parameter D using the following Hamiltonian:

$$H = -2JS_1S_2 + D[(S_1^z)^2 + (S_2^z)^2]$$

In view of the spin anisotropy produced by the ZFS, a Zeeman Hamiltonian that considers both parallel and perpendicular g components has also been added. The full spin Hamiltonian has been solved by a numerical procedure based on a program recently developed by us that allows one to calculate the magnetic properties of spin clusters of arbitrary nuclearity, topology, and anisotropy.⁴⁰

This model allows one to explain the decrease of the magnetic moment at low temperature from a single-ion ZFS parameter $D = 6.3 \text{ cm}^{-1}$ and a J value of 0.83 cm^{-1} .⁴¹ In the fit the two D parameters as well as the two g components have been set to be equal ($g_{\parallel} = g_{\perp}$) in order to reduce the number of parameters. Despite these simplifications, it is clear that this mean D value is completely unrealistic for these metal ions. Thus, the D values found in the quasi-isotropic Fe(III) ion are in the range 0.1 – 0.2 cm^{-1} , while for octahedral Cr(III) ions these values are less than 2 cm^{-1} .⁴² Furthermore, if we plot the theoretical curve of the isothermal magnetization vs the magnetic field at 2 K (Figure 4), as deduced from the above model, we can see that this curve is much lower than the experimental data (curve a in Figure 4). In contrast, a Brillouin function for an $S = 4$ ground state that considers the θ and g values deduced from the fit of the susceptibility data provides a much better description of the experimental curve (curve c in Figure 4).

From the above discussion we can conclude that the low-temperature behavior is dominated by antiferromagnetic intercluster interactions and not by the single-ion anisotropy effects. The presence of small amounts of the antiferromagnetic Fe–Fe and Cr–Cr dimers might also contribute to this decrease. However, if these homometallic dimers are present, that should be at the level of impurities. Note that the ferromagnetic coupling observed in **3** cannot be attributed to intercluster interactions. A definite proof of the intramolecular character of this ferromagnetic coupling comes from the study of the

BEDT–TTF salt containing this dimer.⁴³ In such a salt, the ferromagnetic coupling found is very similar to that of **3** despite the differences found in the dimer–dimer distances and in the way of packing of the dimers.

The X-band ESR spectra (Figure 5) of the three salts agree with the magnetic data. In the chromium (III) derivative (**1**) one observes a quasi-symmetric signal centered at $H = 3400 \text{ G}$ that increases in intensity as the temperature is decreased to reach a maximum at about 15 K. Below this temperature the intensity of the signal decreases very sharply, as can be seen from the integration of the ESR signals, in agreement with the susceptibility results. In the iron (III) derivative (**2**), one observes at room temperature an almost symmetric signal centered at 3300 G, which follows a thermal evolution similar to that observed in **1**. Together with this signal, one observes a weaker and asymmetric signal at low fields (in the range 500–2100 G), which shows a strong temperature dependence. In particular, at low temperature it exhibits an extensive splitting and becomes the dominant signal. This signal is characteristic of isolated octahedral Fe(III) centers having a zero-field splitting around 0.2 cm^{-1} on the spin $S = 5/2$,⁴⁴ thus, it indicates the presence of paramagnetic Fe(III) impurities. Finally, the bimetallic chromium(III)–iron(III) compound **3** exhibits an asymmetric spectrum at room temperature with broad signals in the range 1100–3700 G. This spectrum evolves at low temperature (4.5 K) to give an asymmetric signal in the range 1100–2400 G. Interestingly, no signal attributable to the homometallic species is seen in the region 3000–6000 G, thus confirming the exclusive formation of the Cr(III)–Fe(III) heterometallic dimer in **3**.

In principle it should be possible to determine from which spin state the transitions originate from the temperature variation of the intensities of the EPR spectra of compound **3**. This is not possible here because the lines are very broad because of dipolar broadening and overlapping of different transitions. Furthermore, the presence of an excited $S = 3$ state, which is only at ca. 8.8 cm^{-1} above the ground state, indicates that even at the lowest temperatures reached (down to 4.5 K), this excited spin state is also populated, giving rise to additional transitions. To overcome these problems and to get direct information about the ZFS in the $S = 4$ ground state of this dimer, a more detailed study of **3** in high-field/high-frequency EPR experiments at very low temperatures is required.⁴⁵

The ferromagnetic coupling found in this bimetallic complex deserves an explanation. No precedent of ferromagnetic coupling between these two ions is known, although a ferromagnetic

(41) An approximate way to account for the spin anisotropy effects in this ferromagnetic cluster is by introducing an effective ZFS for the ground $S = 4$ spin state, which is directly connected with that of the single ions. However, such a procedure is only valid when the ground spin state is well separated in energy from the excited spin levels or when the condition $|D| \ll |J|$ is fulfilled. This is not our case, and therefore, the exact model had to be used.

(42) Bencini, A.; Gatteschi, D. In *Transition Metal Chemistry*; Melson, G. A., Figgis, B. N., Eds.; Dekker: New York, 1982; Vol. 8, pp 1–178.

(43) Bérézovsky, B.; Triki, S.; Sala Pala, J.; Coronado, E.; Gómez-García, C. J. Results to be published.

(44) Collison, D.; Powell, A. K. *Inorg. Chem.* **1990**, *29*, 4735.

(45) Barra, A. L.; Brunel, L. C.; Gatteschi, D.; Pardi, L.; Sessoli, R. *Acc. Chem. Res.* **1998**, *31*, 460.

coupling between Cr(III) and Mn(II) has been found in complexes wherein the oxalato ligand acts as a bis(bidentate) ligand bridging the two metal ions. Hence, the origin of this unusual coupling should be the same because Mn(II) is isoelectronic to Fe(III) (high-spin d^5 configuration). It may be attributed to the presence of dominant ferromagnetic exchange pathways, compared to the antiferromagnetic ones. Several kinds of exchange pathways can be distinguished in the three reported complexes: (i) antiferromagnetic pathways coming from $t_{2g}-t_{2g}$ interactions, which occur when the two interacting orbitals contain an unpaired electron each (SOMO-SOMO interaction); (ii) antiferromagnetic pathways coming from e_g-e_g interactions, which occur when the two interacting orbitals contain an unpaired electron each (SOMO-SOMO interaction); (iii) ferromagnetic pathways coming from e_g-e_g interactions, which occur when one orbital containing an unpaired electron interacts with an empty orbital (SOMO-LUMO interaction); (iv) ferromagnetic pathways coming from $t_{2g}-e_g$ interactions, since these orbitals are orthogonal. The $t_{2g}-t_{2g}$ interactions (contribution i) account for the antiferromagnetic coupling observed in the Cr(III)-Cr(III) dimer (d^3-d^3 configuration). The other two complexes contain octahedral Fe(III) in a high-spin configura-

tion; hence, in addition to the $t_{2g}-t_{2g}$ antiferromagnetic pathways, those involving the e_g orbitals are also relevant. The important difference between the two complexes is that in bimetallic Cr(III)-Fe(III) both types of pathways ($t_{2g}-e_g$ and e_g-e_g) are ferromagnetic because they involve contributions iii and iv, while in Fe(III)-Fe(III) the e_g-e_g pathways are antiferromagnetic (contribution ii). Such a difference justifies the different sign of the overall exchange constant in Cr(III)-Fe(III) and Fe(III)-Fe(III) dimers.

Acknowledgment. This work was supported by CNRS (Centre National de la Recherche Scientifique, UMR 6521) and the framework of a French-Spanish Integrated Action (HF96-13 and 98059). F.B. thanks the "Ministère de l'Éducation Nationale, de la Recherche et de la Technologie" for a thesis grant and J.M. C.-J. thanks NOHEMIP TMR Research Network for a postdoctoral grant.

Supporting Information Available: An X-ray crystallographic file in CIF format for the structure determination of **3**. This material is available free of charge via the Internet at <http://pubs.acs.org>.

IC990439W